

First-principles calculation of stacking fault and twin boundary energies of Cr₂Nb

SUKLYUN HONG†, C. L. FU and M. H. YOO

Metals and Ceramics Division, Oak Ridge National Laboratory,
Oak Ridge, TN 37831-6114, USA

[Received 15 July 1998 and accepted 7 June 1999]

ABSTRACT

The stacking fault and twin boundary energies of C15 Cr₂Nb are calculated by the first-principles local-density-functional approach. It is found that the intrinsic and extrinsic stacking fault energies are 116 and 94 mJm⁻², respectively, and the twin boundary energy is 39 mJm⁻². The lower extrinsic stacking fault energy is consistent with the fact that the C36 structure has a lower energy than the C14 structure. The calculated stacking fault energies at 0 K are larger than the experimental values available in the literature. The equilibrium separations between Shockley partials based on the calculated elastic constants and stacking fault energies are also calculated.

§1. INTRODUCTION

For a wide variety of structural applications, Laves phases have some unique properties such as high melting temperature, low density, and high oxidation resistance. Unfortunately, this potential has not been well exploited, largely because of low temperature brittleness due to the lack of plastic deformation. Cr₂Nb, one of the most studied Laves phase compounds, has either the cubic C15 or hexagonal C14 (or C36) structure, which is topologically akin to the face-centred cubic (fcc) (A1) or the hexagonal close-packed (hcp) (A3) structure, or any one of the polytypic phases. The topologically close-packed (TCP) plane of the C15 structure is of the {111} type, and the potential modes of plastic deformation in Cr₂Nb are twelve {111}⟨110⟩ slip systems and twelve {111}⟨112⟩ twin systems. Since each of the TCP units consists of the quadruple atomic layers, the slip, twinning, or stress-induced polytypic transformation will require a coordinated process of atomic motions, such as synchroshear, in order to effect the motion of Shockley partial dislocations.

Among other quantities, the knowledge of stacking fault energy (SFE), γ_{SF} , is necessary to understand the deformation mechanism, since SFE will play an important role in processes such as dislocation dissociation, cross-slip and twinning. First-principles calculations are useful to estimate the energetics of stacking faults (SFs) and understand the interaction between Shockley partials.

Using the linear muffin-tin orbital (LMTO) method, Chu *et al.* (1995a) estimated the intrinsic stacking fault energy of Cr₂Nb from the structural energy difference between the C15 and C14 structures, and obtained $\gamma_{\text{SF}} = 90 \text{ mJm}^{-2}$. On the other

† Present address: Department of Physics, Sejong University, Seoul 143-747, Korea.

hand, Yoshida *et al.* (1995) obtained a value of 8 mJ m^{-2} for SFE from transmission electron microscopy (TEM) observations of extended dislocation nodes at 1623°C . More recently, Kazantzis *et al.* (1996) obtained a value of 25 mJ m^{-2} from TEM observations of extended nodes in Cr_2Nb at 1400 and 1500°C .

In a previous paper (Hong and Fu 1999), we investigated the phase stability of three Laves phases (C15, C14 and C36) of Cr_2Nb . It was found that the C15 phase is the ground-state structure with the lowest energy and the C36 phase is an intermediate state between C15 and C14. These three phases, however, are very close in energy, i.e. within a range of about $60 \text{ meV/formula unit}$ (Hong and Fu 1999) indicating the possibility of low stacking fault energies in this system. In this paper, we report the calculation of SFE using supercell geometry, and an evaluation of the equilibrium separation between Shockley partials using the anisotropic elastic theory.

§2. LAVES STRUCTURES

In describing the structures of Laves phases and their stacking faults and twin boundary, we follow the notations of Hazzledine (1994).

Laves phases have ideal chemical compositions S_2L ; they contain smaller atoms S and larger atoms L in alternate sheets parallel to the TCP planes (i.e. (111) plane for the C15 structure and (0001) plane for the C14 and C36 structures). The main geometric characteristic of Laves phases S_2L is that they consist of two types of atomic stacking sequence, $\alpha\text{A}\alpha$ ($\beta\text{B}\beta$ and $\gamma\text{C}\gamma$) and $\alpha\text{C}\beta$ ($\beta\text{A}\gamma$ and $\gamma\text{B}\alpha$). Here, the Greek letters (α, β, γ) denote the L atoms, while lower case Latin letters (a, b, c) and capital letters (A, B, C) denote the type-1 and type-2 S atoms, respectively. Note that the $\alpha\text{C}\beta$ -type stackings are more closely spaced (in terms of the interlayer spacings). For Cr_2Nb , Latin and Greek letters represent Cr and Nb, respectively.

Figure 1 represents an atomic layer of A atoms based on the hexagonal unit cell on the TCP plane (a Kagome net) which is determined by two lattice vectors

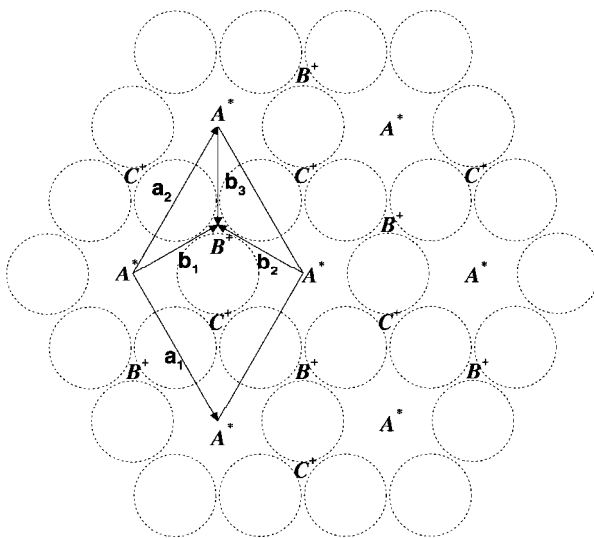
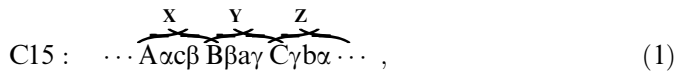
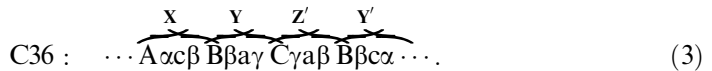


Figure 1. The hexagonal unit cell on the basal planes which is determined by two lattice vectors \mathbf{a}_1 and \mathbf{a}_2 . See the text for details.

$\mathbf{a}_1 = \frac{1}{2}[011]$ and $\mathbf{a}_2 = \frac{1}{2}[110]$. The vectors \mathbf{b}_1 , \mathbf{b}_2 and \mathbf{b}_3 are Shockley partial Burgers vectors of the type $\frac{1}{6}\langle 112 \rangle$ ($\mathbf{b}_1 + \mathbf{b}_2 + \mathbf{b}_3 = 0$). The dotted circles in figure 1 denote A atoms, one of the type-2 S atoms, projected on the (111) plane. Let the centres of hexagonal rings consisting of A atoms be denoted by A^* , and thus the A atoms are placed midway between the lattice points A^* . Similarly, the lattice points B^* and C^* , which determine B and C atoms respectively, can be obtained by the displacement of A^* by \mathbf{b}_1 and $-\mathbf{b}_1$, respectively, on higher or lower planes. Also, we denote the projected points of B^* and C^* onto the plane given in figure 1 as B^+ and C^+ , respectively, which are the saddle points for larger α atoms. Then, the projected atomic positions of α (or a) onto the given plane are at the sites of A^* in figure 1, and the projected positions of β (or b) and γ (or c) are at those of B^+ and C^+ , respectively. Consequently, the TCP C15 structure is defined by repeated XYZ stacking:



where the TCP plane unit X (Y or Z) consists of one single layer of A (B or C) atoms and one triple layer of $\alpha c\beta$ ($\beta a\gamma$ or $\gamma b\alpha$). A synchroshear mechanism was first introduced by Kronberg (1957), and was used to explain the deformation twinning process by several groups (Livingston and Hall 1990, Chu and Pope 1993, Hazzledine 1994). Synchroshearing of the X unit ($A\alpha c\beta$) creates the X' unit ($A\alpha b\gamma$), and similarly for the Y' ($B\beta c\alpha$) and Z' ($C\gamma a\beta$) units. The C14 and C36 Laves phases have repeated $X'Z$ and $XYZ'Y'$ stackings, respectively, as follows:



It can be seen that the primed X' , Y' , Z' units are introduced by synchroshear in order to make sure that TCP structure is maintained in C14 and C36. For example, c and β of the X unit in C15 are synchrosheared by $-\mathbf{b}_2$ and $-\mathbf{b}_1$, respectively, to become b and γ of X' unit. This displacement preserves a close packing between X and Z units in C14.

The stacking sequences for an intrinsic stacking fault (ISF) and an extrinsic stacking fault (ESF) and a twin boundary are given in table 1 in terms of X, Y, Z units. Note that the ISF contains a local C14-like structure in C15, while the ESF contains a local C36-like structure in C15. Figure 2 shows schematic illustrations of an ISF and an ESF obtained from C15 through the synchroshear mechanism: (a) $\text{C15} \rightarrow \text{ISF}$, and (b) $\text{C15} \rightarrow \text{ESF}$. The C15 stacking has a repeated XYZ sequence (no stacking fault). For the ISF, one unit, namely Y, is missing from the C15 XYZ sequence, and X becomes X' by synchroshear (shifts by $-\mathbf{b}_2$ and $-\mathbf{b}_1$ shown in figure 2(a)), while for an ESF a unit Y' is added into the original C15 sequence. For the ESF, two successive synchroshears (two synchro-shifts shown in figure 2(b)) are operative in the $\alpha c\beta$ type to maintain a TCP structure by introducing two primed units, Z' and Y' . Twinned structure is equivalent to a mirror reflection about the X' unit (see table 1).

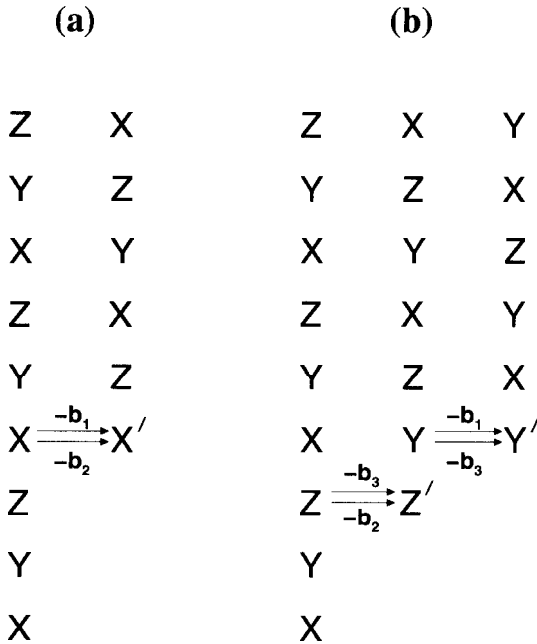


Figure 2. Schematic illustrations of an ISF and an ESF obtained from C15 through the synchroshear mechanism: (a) C15 \rightarrow ISF, and (b) C15 \rightarrow ESF.

Table 1. Stacking sequences of the C15 structure (no stacking fault), intrinsic stacking fault, extrinsic stacking fault, and twin (C15 + C15T) structure.

	Sequence of faults
C15	...XYZXYZXYZ...
Intrinsic stacking fault	...XYZX'ZXYZ...
Extrinsic stacking fault	...XYZXYZ'Y'XYZ...
Twin (C15 + C15T)	...XYZX'Z'Y'X'Z'Y'...

§ 3. STACKING FAULT AND TWIN BOUNDARY ENERGIES

Total-energy calculations for the stacking fault energies of C15 Cr₂Nb are performed using the full-potential linearized augmented plane-wave (FLAPW) method (Wimmer *et al.* 1981) within the local-density approximation. The FLAPW method solves the local-density-functional equations without any shape approximation to the potential or charge density. The atomic positions are relaxed by calculating Hellmann–Feynman forces acting on the atoms.

The supercell geometry is used to obtain the energies of ISF, ESF and twin boundary. In the supercell calculation, we use the experimental lattice constant (6.991 Å) of C15 Cr₂Nb and spacings along **a**₃ axis corresponding to the ideal hcp *c/a* ratio, which gives ~ 4.04 Å for the thickness of each X, Y, Z unit. We consider a supercell containing XYZX'Z for an ISF and XYZXYZ'Y' for an ESF. In these supercells, the separations between ISF and ESF planes are about 20 Å and 28 Å,

respectively. Also, a supercell containing XYZX'Z'Y' ($\sim 24 \text{ \AA}$) is considered for twin boundary. The supercell for twinning contains two twin boundaries in it, thus the separation between twin boundaries is about 12 \AA .

The internal coordinates of each structure are fully relaxed from the ideal positions (defined by the atomic positions of the C15 lattice) by calculating Hellmann–Feynman forces acting on the atoms. The relaxation energies of ISF, ESF, and twin boundary are 41, 20, and 17 mJ m^{-2} , respectively.

The results for the stacking fault and twin boundary energies are given in table 2. It is found that the fault energies are $\gamma_{\text{ISF}} = 116$ and $\gamma_{\text{ESF}} = 94 \text{ mJ m}^{-2}$ for ISF and ESF, respectively, and the twin boundary energy is $\gamma_{\text{T}} = 39 \text{ mJ m}^{-2}$. Since ESFs and ISFs contain local C36-like and C14-like structures, respectively, a lower ESF energy (γ_{ESF}) compared to the ISF energy (γ_{ISF}) is consistent with the fact that the C36 structure has a lower energy than the C14 structure (Hong and Fu 1999).

For comparison, we also calculated the stacking fault and twin boundary energies using the theoretical lattice constant (6.822 \AA). The relaxation energies of ISF, ESF, and twin boundary are 48, 40, and 21 mJ m^{-2} , respectively. It is also found that the fault energies are 140 and 108 mJ m^{-2} for ISF and ESF, respectively, and the twin boundary energy is 52 mJ m^{-2} . The results using the theoretical lattice constant are slightly larger than those using the experimental one.

Although the intrinsic faults are expected to prevail in fcc crystals rather than the extrinsic faults (Hirth and Lothe 1982), extrinsic stacking faults were observed to be dominant in Laves phase Co₂Ti (Allen *et al.* 1972), and Nb-doped HfV₂ (Chu *et al.* 1998). Since the calculated γ_{ESF} is smaller than γ_{ISF} , it is likely that the observed SFs in Cr₂Nb are also of extrinsic type.

We compare our results with others. Chu *et al.* (1995a) obtained $\gamma_{\text{ISF}} = 90 \text{ mJ m}^{-2}$ by an estimation from the structural energy difference between the bulk C14 and C15 structures. This value is close to our value of 116 mJ m^{-2} . On the other hand, Yoshida *et al.* (1995) observed extended dislocation nodes in C15 Cr₂Nb deformed at 1623 K, in which the SFs are bounded by three Shockley partials (of the type $\frac{1}{6}\langle 112 \rangle$) with a radius of curvature of R . They obtained a smaller value of 8 mJ m^{-2} . Note that Chu *et al.* (1995a) re-estimated SFE from the data of Yoshida *et al.* (1995) to obtain $\gamma_{\text{SF}} = 15\text{--}60 \text{ mJ m}^{-2}$. More recently, Kazantzis *et al.* (1996) obtained a value of 25 mJ m^{-2} from TEM observations of extended triple-junction nodes in Cr₂Nb at 1400 and 1500°C. These results are tabulated in table 2.

Our results for SFEs are higher than the experimental results. Certainly, SFE obtained at high temperatures can be expected to be lower than the calculated value at 0 K, which has also been suggested by Kazantzis *et al.* (1996). The unknown image

Table 2. Stacking fault and twin boundary energies for C15 Cr₂Nb, using the experimental lattice constant.

Method	γ_{SF} (mJ m^{-2})	γ_{T} (mJ m^{-2})
This work	116 (intrinsic)	94 (extrinsic) 39
LMTO ^a	90 (intrinsic)	—
Exp ^b	25	—
Exp ^c	> 8	—

^a Chu *et al.* (1995a): estimated from energy difference between C14 and C15.

^b Kazantzis *et al.* (1996): estimated from dislocation triple-junction.

^c Yoshida *et al.* (1995): estimated from dislocation triple-junction.

shift of Shockley partial dislocations can also give an uncertainty in the SFE determination; for example, for SFE in silicon, $\gamma_{\text{SF}} = 30 \text{ erg cm}^{-2}$ has an uncertainty in the range $15 < \gamma_{\text{SF}} < 75 \text{ erg cm}^{-2}$, after taking into account the image shift (Aerts *et al.* 1962). From these points of view, the temperature and image shift effects may be responsible for the difference between our calculated value and experimental results.

Our theoretical calculations on Cr_2Nb were performed for the stoichiometric composition. In experiments, however, some localized variations in chemical composition are possible in polycrystalline compounds. For instance, the two Cr_2Nb alloys investigated by Yoshida *et al.* (1995) were Cr-32. 2% Nb and Cr-34. 0% Nb, in which the second phase particles observed are Cr solid solution in the former and Nb solid solution in the latter. Also, polycrystals used in experiments may have compositions that deviate from the ideal stoichiometry ratio, since the phase region of the C15 Cr_2Nb is relatively large. For example, as mentioned by Hong and Fu (1999), the calculated elastic moduli for the stoichiometry alloy at the experimental lattice constant are very different from the experimental values (Chu *et al.* 1995b) obtained from polycrystals. Therefore, this composition effect can also be partially responsible for the discrepancy between theory and experiment.

The calculated twin boundary energy, $\gamma_{\text{T}} = 39 \text{ mJ m}^{-2}$, at the experimental lattice constant for Cr_2Nb is relatively low, for instance, in comparison to $\gamma_{\text{T}} = 60 \text{ mJ m}^{-2}$ for TiAl of the Ll_0 structure (Fu and Yoo 1990). In view of the energetics of twin nucleation, such a low twin boundary energy suggests a high propensity of twinning in Cr_2Nb . This is consistent with the experimental observations of twinned microstructures in Cr_2Nb , formed due to plastic deformation at elevated temperatures (Yoshida *et al.* 1995) and to the internal stresses resulting from the C14–C15 transformation as well as the thermal contraction differences between Cr solid solution and Cr_2Nb in the two-phase alloy (Kumar and Liu 1997). However, the absence of deformation twinning in Cr_2Nb at low temperatures is not understood. Kinetic aspects of the motion of synchro-Shockley partials need to be elucidated in order to better understand twin formation in the C15 Laves phase.

§4. INTERACTION BETWEEN SHOCKLEY PARTIALS

From the anisotropic elasticity theory (Stroh 1958, Hirth and Lothe 1982) we calculate the equilibrium separation between Shockley partials, using the calculated elastic constants (Hong and Fu 1999) and stacking fault energies.

First, we consider the following case for the ISF:

$$\frac{1}{2}[110] \rightarrow \frac{1}{6}[121] + \text{ISF} + \frac{1}{6}[211], \quad (4)$$

where $\mathbf{B} = \frac{1}{2}[110]$, $\mathbf{b}^{(1)} = \frac{1}{6}[121]$ and $\mathbf{b}^{(2)} = \frac{1}{6}[211]$ correspond to $-\mathbf{a}_2$, \mathbf{b}_3 , and $-\mathbf{b}_1$ in figure 1, respectively. This expression for the formation of an ISF is approximate since the Shockley partial $\mathbf{b}_3 = \frac{1}{6}[121]$ is the sum of two synchro-Shockley partial vectors $-\mathbf{b}_2$ and $-\mathbf{b}_1$, lying in the two successive atomic planes, shown in figure 2 (a). The equilibrium separation between Shockley partials can be obtained through the balance of the attractive force (the surface tension due to the ISF) and the repulsive force (due to elastic interaction between the partials).

The radial and tangential components of the interaction force (per unit length) between two parallel dislocations can be calculated by

$$F_r = f_r / (2\pi r), \quad (5)$$

$$F_\theta = f_\theta / (2\pi r). \quad (6)$$

Here, r is the separation between the two partials of Burgers vectors $\mathbf{b}^{(1)}$ and $\mathbf{b}^{(2)}$, and f_r and f_θ are the radial (in the $\{111\}$ plane) and tangential (out-of-the plane) components of the interaction force constants, which are determined from the anisotropic elasticity theory of dislocations (Stroh 1958). For the dissociation of equation (4), the interaction force constants f_r and f_θ are obtained numerically (Yoo 1987), by (i) letting $\mathbf{b}^{(1)} = \frac{1}{6}[121]$ and $\mathbf{b}^{(2)} = \frac{1}{6}[2\bar{1}\bar{1}]$, (ii) using the experimental lattice constant $a_0 = 6.991 \text{ \AA}$ for C15, and (iii) the calculated elastic constants and γ_{ISF} at experimental lattice constant.

As shown in figure 3, the radial component f_r increases monotonically from $\phi = 0$ (screw) to $\phi = 90^\circ$ (edge), where ϕ is the angle between a dislocation line and the Burgers vector \mathbf{B} . The tangential component f_θ is maximum in magnitude at $\phi = 31^\circ$ and zero at the edge orientation. At $\phi \sim 30^\circ$, the two parallel Shockley partials are inclined at about 60° and 0° to their respective Burgers vectors. This implies that while the repulsive F_r balances the surface tension γ_{SF} (see equation (7) below), the out-of-plane force ($F_\theta = 0.5F_r$ at $\phi = 30^\circ$) promotes cross-slip of the screw Shockley partial and climb of the 60° Shockley partial, most likely onto the (101) plane. This Shockley partial dissociation configuration of the cross-slip and climb combination may lead to a possible mechanism for the thickening process of a twin embryo originating from a mixed ($\phi = 30^\circ$) $\frac{1}{2}[110]$ dislocation.

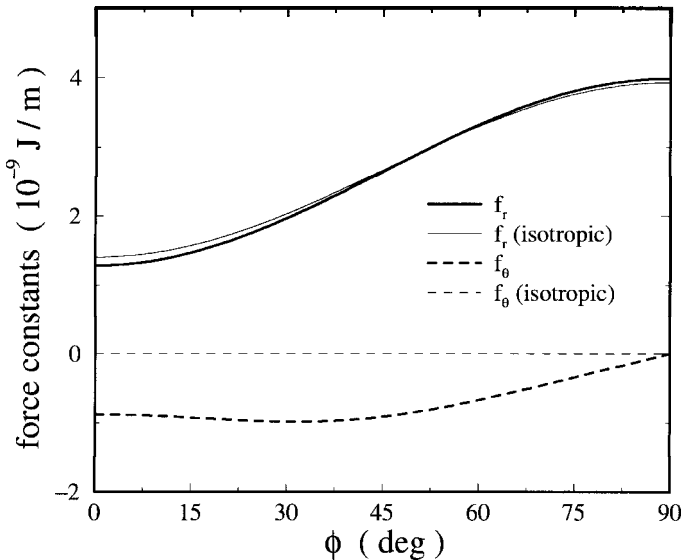


Figure 3. Orientation dependence of the interaction force constants in Cr_2Nb for the ISF-type dissociation, using the results obtained at the experimental lattice constant. ϕ is an angle between a dislocation line and the Burgers vector $\frac{1}{2}[110]$.

The width of the equilibrium separation, w , can be obtained from

$$\gamma_{\text{SF}} = F_r = f_r/(2\pi w), \quad (7)$$

$$w = f_r/(2\pi\gamma_{\text{SF}}). \quad (8)$$

The separation is $w_s = 17.6 \text{ \AA}$ for the $\mathbf{B} = \frac{1}{2}[110]$ screw dislocation, and $w_e = 54.7 \text{ \AA}$ for the edge dislocation. These results are shown in table 3, together with those in the isotropic case (discussed below). Also, the results using γ_{ESF} and the experimental result are tabulated.

For the isotropic case, the equilibrium separation w is given by a simple formula (Hirth and Lothe 1982):

$$w = \frac{Gb^2}{8\pi\gamma_{\text{SF}}} \frac{2-\nu}{1-\nu} \left(1 - \frac{2\nu \cos 2\phi}{2-\nu} \right). \quad (9)$$

Here, $b = |\mathbf{b}^{(1)}| = |\mathbf{b}^{(2)}| = a_0/6^{1/2}$. The Hill's average values of shear modulus and the Poisson's ratio are $G = 50.0 \text{ GPa}$ and $\nu = 0.383$, respectively. Using γ_{ISF} , it is found that $w_s = 19.3 \text{ \AA}$ and $w_e = 53.9 \text{ \AA}$. As given in table 3, the results in anisotropic and isotropic cases are rather close, because the shear anisotropy of Cr₂Nb is moderate, $A = 1.45$ (Hong and Fu 1999), compared to the isotropic case ($A = 1$).

The radial component f_r of the isotropic case is very close to that of the anisotropic one, whereas its tangential component f_θ is exactly zero (figure 3). While the anisotropic corrections to f_r and hence to w in equation (9) are very small, the anisotropic tangential component of the elastic interaction force is quite large; for instance, $f_\theta/f_r \sim 0.7$ at $\phi = 0$. This indicates that cross-slip of $\frac{1}{2}[110]$ dislocation is difficult in Cr₂Nb because of a large constriction energy for the Shockley partials that include the non-radial component of the interaction energy.

Next, let us consider the ESF case:

$$\frac{1}{2}[110] \rightarrow \frac{1}{6}[121] + \frac{1}{6}[112] + \text{ESF} + \frac{1}{6}[211] + \frac{1}{6}[112] \quad (10)$$

$$\approx \frac{1}{6}[2\bar{1}\bar{1}] + \text{ESF} + \frac{1}{6}[1\bar{2}1]. \quad (11)$$

To calculate the width of the ESF, we approximate two Shockley partials on two successive TCP units on either side of the ESF by a single Shockley partial (as in the ISF case), and use the same formulas for the ISF. In other words, the only difference

Table 3. Equilibrium separation between Shockley particles bounding an ISF and an ESF, using the results obtained at experimental lattice constant. w_s and w_e are the width for screw and edge dislocations, respectively. The numbers are in angstroms.

		w_s (screw)		w_e (edge)	
		ISF	ESF	ISF	ESF
Theory ($T = 0 \text{ K}$)	Anisotropic	18	22	55	68
	Isotropic	19	24	54	67
Exp ^a ($T = 1400^\circ\text{C}$)		99		—	

^a Kazantzis *et al.* (1996): measured from the ribbon after the correction for image shift and projection effects.

between ISF and ESF in the calculation of separation w is that the stacking fault energy used in the formulas is of intrinsic or extrinsic type. Using γ_{ESF} , it is found that $w_s = 21.7 \text{ \AA}$ and $w_e = 67.5 \text{ \AA}$ for the anisotropic case (table 3). For the isotropic case, they are $w_s = 24.4$ and $w_e = 66.5 \text{ \AA}$. As mentioned, the results of both anisotropic and isotropic cases are very close. Since γ_{ESF} is not much different from γ_{ISF} , the force constants f_r and f_θ using γ_{ESF} are expected to be similar to those in figure 3 using γ_{ISF} .

On the other hand, we consider the separation between partials by using the theoretical lattice constant. For the ISF, the separation is $w_s = 17.1 \text{ \AA}$ and $w_e = 53.5 \text{ \AA}$ for the anisotropic case, while $w_s = 18.7 \text{ \AA}$ and $w_e = 52.8 \text{ \AA}$ for the isotropic case. For the ESF, the separation is $w_s = 22.2 \text{ \AA}$ and $w_e = 69.4 \text{ \AA}$ for the anisotropic case, while $w_s = 24.2 \text{ \AA}$ and $w_e = 68.4 \text{ \AA}$ for the isotropic case. It can be seen that the separations are very close when using both experimental and theoretical lattice constants.

Kazantzis *et al.* (1996) measured, at $T = 1400^\circ\text{C}$, the width of the ribbon (separation between two parallel partial dislocations) as 99 \AA after correction for image shift and projection effects. Note that they also obtained a different value of $w_s = 82 \text{ \AA}$ for the width using equation (9) with $\gamma_{\text{SF}} = 25 \text{ mJm}^{-2}$, which was estimated from the measured curvature of R in extended dislocation nodes and the temperature-corrected shear modulus. Compared with the experimental result at high temperatures, our results for the separation between partials are very small.

§ 5. SUMMARY

We performed first-principles total-energy calculations to obtain stacking fault and twin boundary energies. The intrinsic and extrinsic stacking fault energies were calculated to be 116 and 94 mJm^{-2} , respectively, and the twin boundary energy was 39 mJm^{-2} . The calculated stacking fault energies are larger than the available experimental data, measured at high temperatures. We also calculated the equilibrium separations between Shockley partials using the calculated elastic constants and stacking fault energies. Our results of the equilibrium separations are very small compared with the experimental results reported at high temperatures. This discrepancy may be due to temperature and/or composition and image shift effects.

ACKNOWLEDGEMENTS

The research was sponsored by the Division of Materials Sciences, Office of Basic Energy Sciences, US Department of Energy under contract DE-AC05-96OR22464 with Lockheed Martin Energy Research Corporation.

REFERENCES

- AERTS, E., DELAVIGNETTE, P., SIEMS, R., and AMELINCKX, S., 1962, *J. appl. Phys.*, **33**, 3078.
 ALLEN, C. W., DELAVIGNETTE, P., and AMELINCKX, S., 1972, *Phys. status solidi* (a), **9**, 237.
 CHU, F., ORMECI, A. H., MITCHELL, T. E., WILLS, J. M., THOMA, D. J., ALBERS, R. C., and CHEN, S. P., 1995a, *Phil. Mag. Lett.*, **72**, 147.
 CHU, F., HE, Y., THOMA, D. J., and MITCHELL, T. E., 1995b, *Scripta metall. mater.*, **33**, 1295.
 CHU, F., LU, Y.-C., KOTULA, P. G., MITCHELL, T. E., and THOMA, D. J., 1998, *Phil. Mag. A*, **77**, 941.

- CHU, F., and POPE, D. P., 1993, *High-Temperature Ordered Intermetallic Alloys V, Materials Research Society Symposium Proceedings*, Vol. 288, edited by I. Baker, R. Darolia, J. D. Whittenberger and M. H. Yoo (Materials Research Society), p. 561.
- FU, C. L., and YOO, M. H., 1990, *Phil. Mag. Lett.*, **62**, 159.
- HAZZLEDINE, P. M., 1994, *Twining in Advanced Materials*, edited by M. H. Yoo and M. Wuttig (The Minerals, Metals & Materials Society), p. 403.
- HAZZLEDINE, P. M., and PIROUZ, P., 1993, *Scripta metall. mater.*, **28**, 1277.
- HIRTH, J. P., and LOTHE, J., 1982, *Theory of Dislocations* (New York: Wiley).
- HONG, S., and FU, C. L., 1999, *Intermetallics*, **7**, 5.
- KAZANTZIS, A. V., AINDOW, M., and JONES, I. P., 1996, *Phil. Mag. Lett.*, **74**, 129.
- KRONBERG, M. L., 1957, *Acta metall.*, **5**, 507.
- KUMAR, K. S., and LIU, C. T., 1997, *Acta mater.*, **45**, 3671.
- LIVINGSTON, J. D., and HALL, E. L., 1990, *J. mater. Res.*, **5**, 5.
- STROH, A. N., 1958, *Phil. Mag.*, **3**, 625.
- WIMMER, E., KRAKAUER, H., WEINERT, M., and FREEMAN, A. J., 1981, *Phys. Rev. B*, **24**, 864.
- YOO, M. H., 1987, *Acta metall.*, **35**, 1559.
- YOSHIDA, M., TAKASUGI, T., and HANADA, S., 1995, *High-Temperature Ordered Intermetallic Alloys VI, Materials Research Society Symposium Proceedings*, Vol. 364, edited by J. Horton, I. Baker, S. Hanada, R. D. Noebe and D. S. Schwartz (Materials Research Society), p. 1395.